



OPEN

Valorisation of agricultural biomass-ash with CO₂

Colin D. Hills^{1✉}, Nimisha Tripathi^{1✉}, Raj S. Singh², Paula J. Carey¹ & Florence Lowry¹

This work is part of a study of different types of plant-based biomass to elucidate their capacity for valorisation via a managed carbonation step involving gaseous carbon dioxide (CO₂). The perspectives for broader biomass waste valorisation was reviewed, followed by a proposed closed-loop process for the valorisation of wood in earlier works. The present work newly focusses on combining agricultural biomass with mineralised CO₂. Here, the reactivity of selected agricultural biomass ashes with CO₂ and their ability to be bound by mineralised carbonate in a hardened product is examined. Three categories of agricultural biomass residues, including shell, fibre and soft peel, were incinerated at 900 ± 25 °C. The biomass ashes were moistened (10% w/w) and moulded into cylindrical samples and exposed to 100% CO₂ gas at 50% RH for 24 h, during which they cemented into hardened monolithic products. The calcia in ashes formed a negative relationship with ash yield and the microstructure of the carbonate-cementing phase was distinct and related to the particular biomass feedstock. This work shows that in common with woody biomass residues, carbonated agricultural biomass ash-based monoliths have potential as novel low-carbon construction products.

This paper discusses environmental issues that are of relevance to the sustainable use of resources and protection of the environment. By re-using abundantly available agricultural biomass residues, and by reducing the amount of cement used in construction and their associated carbon emissions, significant potential sustainability gains can be realised. In consideration of this, a low carbon management option for biomass residues is proposed.

Agricultural activities generate huge volumes of biomass residues, with crop derived waste accounting for 94% of global biomass production¹. These include cereals (wheat, rice, maize, and barley), sugarcane, soybean, and some oil crops, fruits, vegetables, roots and tubers, and sugar beet¹. These residues are expected to increase as the world's population exceeds 11 Billion by 2,100².

It is estimated that globally 140 Gt of agricultural residues are generated each year^{3,4}. According to Lal (2019)⁵, the total annual amount of crop residue produced globally is estimated at 2.8 Gt for cereal crops, 3.1 Gt for 17 major cereals and legumes, and 3.8 Gt for 27 common food crops. The IEA CCC (2015)⁶ reports the global resource for unexploited cereal crop residues amounts to 517 Mt.

The FAO (2002)⁷ projects that from 1999 to 2030, the agricultural sector of developing countries will increase by 13% or 120 M ha. Predictions for global cereal yield suggest an increase in the range 0.9% per annum over the period 2005/2007–2050, continuing a trend of long-term declining yield growth (20 y average yield increase declined from ~ 3% pa in 1982, to ~ 1% by 2005)^{8,9}. The intensification of agricultural and increased crop yield (producing more per unit of land) will undoubtedly raise crop residue production¹⁰.

A positive correlation exists between crop-residue availability and its production (e.g. the ratio of the amount of straw to grain, as in the case of cereals), based on the residue-to-crop ratio in a given country, region or at global scale^{11–14}. Geographical location may also influence the crop residue to production relationship¹⁵. Some studies assume a directly proportional relationship between the amount of crop residue and crop yield (production per area unit), rather than total crop production^{16,17}. The recoverable fraction (i.e. crop yield) could be as much as 25% of harvested residue and 90% as the processing residue^{18,19}.

Agricultural biomass wastes and residues from primary production are found in the form of crops stalks, leaves, roots, fruit peels, seeds and nut shells. These wastes are not consumed directly as food or other by-products and their managed disposal is very important. Globally, 66% of the residual plant biomass comes from cereal straw (stem, leaf, and sheath material), with over 60% residues produced in low-income countries²⁰. The major crops, including wheat, maize, rice, soybean, barley, rape seed, sugar cane, sugar beet have an annual global

¹Indo:UK Centre for Environment Research and Innovation, University of Greenwich, Chatham Maritime, Kent, UK. ²Indo:UK Centre for Environment Research and Innovation, CSIR-Central Institute of Mining and Fuel Research, Dhanbad, India. ✉email: c.d.hills@gre.ac.uk; n.tripathi@gre.ac.uk

	Production (Mt)	References	
Fruits			
Citrus	124.7	83	
Banana	114.1		
Apple	84.6		
Grapes	74.5		
Mango, Mangosteen and Guava	45.2		
Pineapple	25.4		
Vegetables			
Potato	388		
Tomato	171		
Cabbage and other Brassicas	71.8		
Carrot and Turnip	38.8		
Cauliflower and Broccoli	24.2		
Peas	17.4		
Residues (from peeling and processing of fruit and vegetables) (% w/w, total weight)			
Citrus fruit	50	84–86	
Banana	35		
Grapes	20		
Potato	15		
Jackfruit	50–70		

Table 1. Global production of fruits, vegetables and residues.

residue potential of about 5Gt¹⁷. Table 1 shows the production of fruit and vegetable and other residues; the former two being particularly in increasing demand, as the global population grows.

Traditionally, root and tuber crops are the mainstay of food in many countries, providing 45% of the world's carbohydrate supply, as well as for animal feedstocks and industrial products (e.g., starch, distilled spirits etc.). The projected annual global demand for root and tuber crops per capita is expected to increase from 69 to 75 kg/y from 1999 to 2050. The major root and tuber crops are potato, sweet potato, cassava and yam are key to maintaining food security and the promotion of better livelihoods through value chain opportunities²¹. Cassava, for example, has potential for biofuel production, which is projected to increase from the 1 Mt/y in 2005, to around 8 Mt/y by 2050. In China, the use of cassava as a feedstock for biofuel production is projected to increase from 0.4% in 2005 to 1.8% by 2050^{22,23}, suggesting that demand could be even higher. The tentative forecast for world cassava production for 2015 was 289 Mt, 0.5 Mt more than 2014. However, in sub-Saharan Africa production in 2015 was 163 Mt, showing a decline of 3 Mt from 2014, primarily resulting from adverse weather conditions²⁴.

Nuts and drupes (fleshy thin-skinned fruit with a central stone and seed) are another important food source. Globally, 72% of total global drupe production involved coconut and mango, and the remaining 28% from nuts (almonds, pistachio and walnuts), stone fruit (cherries, peach, plum and nectarines) and olives, originating in Poland, Turkey, Japan, Spain, Italy and Greece^{25,26}. The global annual availability of drupe endocarp biomass (residue) is primarily driven by coconut production and ranges from 24 to 31 Mt/y^{26,27}. The other substantial residue is generated from the cashew apples (i.e. the juicy swollen pedicel). About 95% of the global cashew apple crop is allowed to rot²⁸, and in India 98% (3.9 Mt/y) is lost this way²⁹.

As indicated above, the global use of hydraulic cement, which is consumed in bulk, is second only to water. In 2018, consumption reached 4.1 Gt³⁰, and is projected to rise to 4.8 Gt/y by 2030³¹. China is the largest cement producing country (about 60% of global production) followed by India (7%). To mitigate the impact of cement production, associated emissions require management by, for example, carbon capture, utilization and storage (CCUS) technologies and the use of lower-temperature (lower carbon intensive) alternative clinkers or both. As discussed in the present work, the use of agricultural wastes may have a role to play.

Challenges/issues from an environmental perspective. Biomass and their residues are low-cost voluminous material resources that are generally environmentally benign, often being returned to the soil as an enriching media. Greater than 2 Gt of unused crop residues are dumped in municipal landfills or burned by households in developing countries³². These activities contribute to 18% of total global CO₂ emissions^{33–36}.

The use of biomass waste to produce energy and other products is of mounting interest. In this regard, the energy potential of residues, in 2050, has been estimated to be in a range of 15–280 EJ yr⁻¹ globally^{37–40}. However, this estimation of biomass residues generated or their potential for alternative uses is approximate⁴¹. As such, the global availability of crop residues has been re-examined by Tripathi et al. (2019)³⁶.

In most developed and developing countries, the collection, recycling and sustainable disposal of the increasing quantities of biomass and other solid wastes are the major challenges. Their conversion into energy and other products can reduce environmental harms and generate much needed value, particularly in developing countries with large quantities of available biomass.

By far, the greatest use of biomass wastes has been as an energy source by direct combustion of wood and crop residues⁴² and in developing countries, biomass is dominantly used as a fuel in open fires for cooking and heating^{43,44}. Globally, nearly three billion people rely on biomass-based fuels sourced from wood or charcoal for cooking and heating⁴⁵. However, for biomass-based power generation, the EU and USA account for most⁴⁶. Biomass burned in Europe to produce energy is projected to contribute 20% of the European renewable energy target by 2020⁴⁷. As biomass incineration and pyrolysis generates substantial amounts of ash and CO₂, innovative management strategies that can incorporate both are timely. Ideally, biomass ash should be returned to land as an enrichment, but energy from waste generates large volumes of ash that fall within waste management regulations, necessitating management by for example, landfilling. These landfill 'deposits' are a relatively consistent potential resource for manufactured products.

Globally, the demand for 'carbon efficient' management solutions to minimise CO₂ emissions and utilise waste is increasing⁴⁸. The Paris agreement recommendations are for immediate action to keep the global increase in temperatures below 1.5 °C⁴⁹. As carbon capture and storage (CCS) in the geosphere is slow to mature, there is a need to explore carbon capture and utilisation (CCU) for the management of point source CO₂ emissions. Indeed, emerging CCU technologies offer significant opportunities for the management of biomass waste coupled with value-addition and CO₂ emissions reductions (hence the acronym, CCUS).

As a recent example, in November 2019, in Delhi and its adjacent major state, Punjab, suffered record levels of smog and poor air quality. The major contributor (about 50%) was stubble burning by the farmers. In one single day 5,953 fires burned and a monthly total of 31,267 fires was recorded⁵⁰.

As mentioned, the production of cement has a high associated carbon footprint, as calcination generates large amount of CO₂ gas (approximately 650–750 kg CO₂/t of cement produced). Some 7% of worldwide greenhouse gas emissions are attributed to cement production⁵¹.

During 2014–2017, the IEA (2019)³⁰ reported an annual increase of 0.5% in clinker-to-cement ratio, resulting into an increase of 0.3%/y in the direct CO₂ intensity of cement production. This report emphasised the need for an annual decline in emissions of 0.7% by 2030 and deployment of CCUS-based technologies to achieve a sustainable emissions reduction scenario.

An approach that can combine biomass waste management with a reduction of cement production-related emissions is described below. Thus, the present work involves the transformation of CO₂ into mineral carbonates on biomass ash, in a way previously described for other thermal or mineral wastes^{52,53}.

Materials and methods

In the present study, biomass residues are categorised as: shell, fiber and soft peel wastes. The biomass residues derived from shell include cobnut, coconut, walnut, almond and peanut; fiber includes jute (hemp), flax, barley straw, hay, and husks from rice and sugarcane; and soft peel includes sweet lime, orange, banana, yam, cassava, potato and pomegranate. The biomass residues described were sourced from India, Africa and the UK.

The residues were ashed in a muffle furnace at 900 ± 25 °C, over 4 h and then examined for (1) selected physical properties (e.g. particle size, bulk density, surface area and ash content) and (2) chemical composition (total carbon, elemental and phase-chemistry).

The particle size distribution of ashes was measured by laser diffraction analysis (Malvern Mastersizer MS2000) and bulk density by loose compaction in cylindrical holders (expressed as kg/m³). The surface area was determined (Micromeritics Gemini V2.00), and total carbon was analysed by CHN analysis (FLASH EA 1112 Series). The bulk elemental composition was determined by X-ray fluorescence spectrometry (Philips LW1400 and XRFWIN software).

The biomass ashes were moistened (20% w/w, total weight) to examine their reactivity to pure CO₂ at a pressure of ~2 bar. The ashes were exposed to CO₂ for four-separate cycles in a closed pressurised carbonation chamber, with the first three cycles extending to one hour each, and the fourth cycle being 24 h. The uptake of CO₂ in ashes was determined on weight gain (% w/w, total weight) basis. This approach was taken as the results obtained correlate closely to those experienced during the carbonation of wastes in commercial facilities^{36,54}.

Product development and characterisation. For the production of monolithic specimens, biomass ashes were moistened (10% w/w, total weight) using a dropper followed by thorough hand-mixing, before being cast as small monolithic cylinders (7 mm × 7 mm—a similar size to manufactured carbonated aggregates). The casting process involved placing the moist ash in the mould followed by hand tamping and the top surface being struck, using a straight-sided spatula. Cylinders in their moulds were placed in a closed curing chamber containing pure CO₂ at 50% RH. After 1 h, samples were de-moulded, and returned to the CO₂ chamber to complete their cycle of 24 h exposure. Non-carbonated samples were treated similarly, but without exposure to CO₂ and were regularly too fragile to demould after curing in air had been completed.

Some of the biomass ashes (including wood biomass ashes) are discussed in Tripathi and Hills et al. 2020⁵⁴. As mentioned earlier, it was necessary to add Portland cement raw biomass waste to provide a reference point, as Portland cement is a commonly used hydraulic cementitious binder. Raw biomass with and without Portland cement was mixed with fine sand (used as an inert mineral filler to change particle size distribution) and then cast into larger monolithic cylinders (3.4 cm × 3.4 cm) (Table 6). It should be emphasised that the Portland cement was used here for its ability to react with CO₂ gas and produce calcium carbonate rather than its normal use as a hydraulic medium. Cylinders were cured in pure CO₂ for one week.

Assessment of CO₂ uptake and strength in valorised biomass products. The CO₂ uptake by the monoliths was calculated on weight gain (% w/w, total weight) basis and also by CHN analysis. The strength of

these monolithic products was evaluated by applying a force until the cylinders failed. The strength was calculated by using the Eq. (1):

$$\sigma_c = \frac{2.8F_c}{\pi dm^2} \quad (1)$$

where σ_c is the compressive strength in megapascals, F_c is the fracture load in kilonewtons, A_m is the mean area of the cylinder, and dm is the mean diameter of the cylinder.

For each batch of carbonated cylinders, the average strength was calculated from the load recorded at failure, with the three axes of each cylinder being measured using digital callipers (Mecmesin MFG250).

The water resistance of carbonated 'ash only' monoliths was monitored by immersing them in tap water for 30 days to investigate their water sensitivity.

The biomass ashes and resultant carbonate-cemented products were investigated by X-Ray diffractometry and electron microscopy.

The biomass ashes without and with CO₂ exposure were analysed with a Siemens D500 diffractometer, fitted with a Siemens K710 generator using 40 kV voltage and 40 mA current, between 5° and 65° 2 θ . The interpretation of diffractograms was aided by DIFFRAC^{plus} EVA software (Bruker AXS) and Rietveld refinement.

The capture of back-scattered electron micrographs augmented by EDAX analysis (JEOL JSM-5310LV, Oxford Instruments Energy Dispersive Spectrometer-EDAX) was performed on polished resin blocks, for both carbonated and reference (no-carbonated) biomass-ash products.

Results and discussion

By combining biomass residues (both raw and ashed) and CO₂ gas into solid monolithic products a potential future 'zero waste' option for these residues is established. Indeed, 4 individual biomass wastes presented in this work have been recently examined by the authors⁵⁴ and are used here as reference residues.

The potential of biomass waste with the *right* chemical and mineralogical composition to react with gaseous CO₂ is harnessed to develop products that are analogous to those made with hydraulic cement. The manufactured products include those hardened by 'ash only' and where ash was used as a partial replacement for cement. Both approaches were used to encapsulate raw biomass in different combinations.

The potential for further innovation including the integration of a direct flue-gas capture and mineralisation step could have significant environmental benefits, not least as this 'circular economic' approach will reduce both the landfilling of biomass waste/residue and gaseous emissions, whilst protecting virgin resources. An offsetting of CO₂ via the replacement of hydraulic cement will be a further added benefit. This 'offset' is of particular importance as we have seen, the cement industry is growing at the rate of about 2.5% pa generating 39.3 ± 2.4 Gt during the period 1928–2016, with 90% of this evolved since 1990⁵⁵.

Physical, chemical and mineralogical characteristics of biomass residues. The physical and chemical characteristics of the biomass residues as received, and their ashes are given in Table 2. The surface area of raw fibres was higher compared to shell and soft peel with the later having the lowest values recorded. The ashes from soft peel wastes have a higher surface porosity than most of the ash generated from fibre-waste. The particle size distribution of ashes was specific to the individual biomass feedstock (Table 2). The size range of ash particle size was 3–39 μ m for soft peel, 14–52 μ m for shell and 1.21–45 μ m for fibre-derived ashes.

The total carbon content of ashes varied with some soft peel waste giving a higher yield. A similar trend was observed for shell ash. The carbon content in all the fibre-derived ashes, except rice husk, was generally less variable and within in the same range (Table 2).

The oxide equivalent composition of ashes is given in Table 3. Walnut shell, jute (hemp) and sweet lime ashes had the highest CaO content in their respective biomass categories. Calcia is the key mineral indicator of the potential CO₂ reactivity of these ashes. It should be noted that coconut shell ash, which had low ash content (0.3% w/w, total weight) was partially characterised as a potential candidate ash, but due to the lack of sample could not be fully evaluated in this study.

Once manufactured, the carbonated 'ash only' monolithic specimens remained intact after immersion in water for 30 days, with no signs of physical degradation, except for the banana peel ash where some swelling and micro-cracking was observed; this was attributed to incomplete carbonation and the presence of CaO, which hydrated forming portlandite (detected by XRD) led to moisture-induced expansion.

Ash content and CO₂ reactivity. The major and minor elements including Al, Ca, Cl, Fe, O, K, Mg, P, Na, S, Mn, Si and Ti in biomass are the major ash forming elements. These elements are generally found in decreasing order of abundance⁵⁶:

$$O > Ca > K > Si > Mg > Al > Cl > P > Fe > Na > S > Mn > Ti$$

Vassilev et al. (2017)⁵⁶ reported a negative relationship between calcia and ash content in individual species of wood, but not agricultural biomass where a positive relationship was identified. These observations are not universally applicable to woody biomass examined in our as yet unpublished work (where some positive relationships were found), and for the agricultural biomass examined here (where some negative relationships were observed). Some of the soft peel wastes had both high calcia and ash contents (Tables 2 and 3), indicating biomass waste is complex and heterogeneous in nature. By way of example, citrus fruit peels, including orange and sweet lime, have a 'high' calcia content; an observation also reported by Sweitzer (2018)⁵⁷. The ash yield from citrus peel is higher than other 'low' calcia containing fruit peel -an observation also reported by Vassilev et al. (2017)⁵⁶.

Type of biomass	Biomass ash	Ash content (%)	Ash particle size D ₅₀ (μm)	Total carbon in ash (g/kg)	Surface area (m ² /g)	
					Raw biomass (m ² /g)	Biomass ash (m ² /g)
Shell	Cobnut shell	0.70	18.14	8.54	0.93	2.61
	Coconut shell	0.31	–	5.18	1.99	5.87
	Walnut shell	0.30	52.3	12.41	0.63	1.77
	Almond shell	0.94	24.10	8.58	0.36	1.43
	Peanut shell	1.38	13.87	9.62	1.43	3.13
Fibre	Jute (hemp)	0.96	45.38	5.09	1.42	2.71
	Flax	1.41	28.33	7.45	1.52	3.94
	Straw (barley)	3.17	11.22	5.74	1.35	2.62
	Hay	1.98	16.22	6.25	1.14	3.50
	Rice husk	5.08	1.21	10.43	1.76	2.79
	Coconut husk (coir)	0.80	6.86	5.18	1.48	1.97
	Sugarcane husk	4.64	9.91	5.78	1.41	1.59
Soft peel	Sweet lime	3.06	43.20	17.28	0.93	2.99
	Banana	3.80	2.90	8.70	0.33	2.32
	Yam	6.36	33.5	10.86	0.72	0.85
	Cassava	5.23	37.0	5.31	0.88	1.67
	Potato	4.22	3.40	7.77	0.31	5.47
	Pomegranate	1.45	15.59	10.07	0.28	1.92
	Orange	3.10	38.83	7.92	0.64	1.25

Table 2. Particle size and BET surface area of raw biomass and their ash.

Type of biomass	Biomass Ash	K ₂ O	CaO	SO ₃	MgO	SiO ₂	P ₂ O ₅	Al ₂ O ₃	Na ₂ O	Fe ₂ O ₃	Cl	SrO	MnO	TiO ₂	ZnO
Shell	Cobnut shell	21.2	18.1	1.1	3.6	8.8	2.8	1.1	0.4	1.5	0.1	0.04	0.4	0.1	0.03
	Walnut shell	4.1	52.3	1.1	5.1	4.4	2.5	1.0	4.3	2.2	0.9	–	0.2	0.06	0.04
	Almond shell	24.4	24.1	14.4	3.4	4.2	3.8	1.1	0.9	0.7	–	0.5	0.08	0.04	0.02
	Peanut shell	21.8	13.9	12.4	11.7	7.8	3.1	2.4	1.8	1.6	0.6	0.3	0.2	0.1	0.04
Fibre	Jute (hemp)	10.2	45.4	2.5	2.6	5.2	2.1	0.7	0.2	1.2	–	0.09	0.09	–	0.04
	Flax	8.4	28.3	3.6	3.0	8.4	3.2	2.4	0.3	2.1	–	0.05	0.2	0.3	0.05
	Straw (barley)	23.7	11.2	3.1	1.3	26.0	1.8	1.1	1.1	0.4	0.4	0.03	0.1	–	0.03
	Hay	13.4	16.2	4.5	2.1	21.6	5.5	0.5	1.3	0.4	0.08	0.04	0.4	0.04	0.06
	Rice husk	3.6	1.2	0.08	2.5	68.2	6.7	0.4	0.1	0.4	–	0.05	0.1	0.03	0.02
	Coconut husk (coir)	14.5	6.9	3.6	1.0	18.1	1.9	1.8	2.0	2.1	17.0	0.1	0.05	0.2	0.03
	Sugarcane husk	9.2	9.9	5.1	4.3	25.6	3.4	3.6	0.8	2.7	0.08	0.03	0.06	0.3	0.03
Soft peel	Sweet lime	15.9	43.2	2.8	3.1	2.5	2.4	0.4	0.6	0.4	–	0.03	0.04	–	0.02
	Banana	36.5	2.9	1.2	0.7	7.2	2.7	0.4	0.1	0.3	1.9	0.06	0.07	–	0.02
	Yam	51.8	5.6	4.1	5.4	10.1	20.9	0	0.07	1.1	0	0.04	0.2	0.3	0.1
	Potato	27.8	3.4	2.2	0.07	4.1	3.6	0.6	0.4	0.3	0.2	0.09	0.02	–	0.04
	Cassava peel	15.2	17.6	5.4	5.9	35.2	5.7	9.8	0.2	2.5	0.07	0.1	0.8	0.9	0.2
	Pomegranate	23.6	15.6	6.3	3.7	1.6	1.4	0.5	0.5	0.4	0.2	0.2	0.04	0.04	0.03
	Orange	21.8	38.8	3.9	3.7	3.1	4.5	0.8	1.1	0.3	–	0.2	0.04	–	0.03
	Cassava pulp	6.4	37.8	3.3	16.3	4.4	2.7	0.3	0.8	0.5	–	0.2	0.5	–	0.1

Table 3. Mineralogical composition of agricultural biomass ashes (% w/w, total weight). Note: Over 10% is good for reasonable uptake.

The fibres, jute (hemp) and flax, had low ash and high calcia content. This relationship is contrary to Vassilev et al. (2017)⁵⁶ observations and may be attributed to these bast fibres having pectin and calcium ions ‘gluing’ constituent fibres together⁵⁸. On the other hand, rice and sugarcane husk presented high ash and low calcia contents. Vassilev et al. (2017)⁵⁶ reported extremely low CaO contents in rice husk, due to high ash yield; data that supports the negative CaO:ash yield-relationship discussed above.

Some shell-derived ashes were calcia rich, up to 52% w/w (total weight), with walnut as an example (Table 3). However, the ash content of shell waste was low, following the negative relationship previously described⁵⁶. That

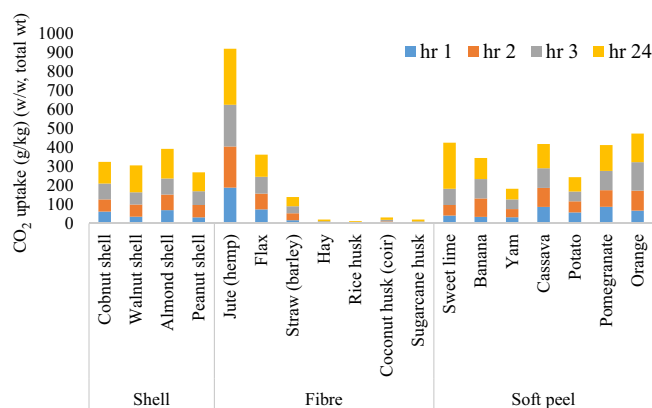


Figure 1. Cumulative CO₂ uptake (w/w, total weight) in agricultural biomass ashes after 4 carbonation cycles.

said, the enrichment pattern is opposite to these previously reported findings that reported calcia depleted ash upon burning, which was not observed in our study.

The relationship observed in our work between ash yield and calcia content can be explained by the observation that a high ash results from combustion of biomass particularly enriched in silica/silicates. The ashes abundant in Ca, Cl, Fe, K, Mg, Na, P, S, chloride, sulphate, carbonate and phosphate tend to be of lower yield -also noted by Vassilev et al. (2013, 2014)^{59,60}.

The ash arising from herbaceous biomass has been shown to vary with the part of the plant being combusted^{61,62}; with grains having a lower ash content than their straw⁶³. Other factors related to the ash content of agricultural biomass include:

1. the loss of nutrients from plants, as a wash-effect by precipitation or delayed harvest⁶⁴,
2. the type of soil used for growing plants⁶⁵, and
3. the season they are grown in, especially for grass species⁶¹.

As observed in the present study, some fruit peel, shell and fibre-biomass yielded higher calcia containing ashes (see Table 3); the key mineral indicator of CO₂ reactivity.

CO₂ uptake in biomass ash and their products

Biomass ashes. As mentioned, CO₂-reactive biomass ashes represent a potential resource for the manufacture of value-added products. However, in an industrialised setting involving, e.g., energy from biomass waste, ashes will be classed as waste and, therefore, to meet 'end of waste' regulations (and to be legally declared as a product), carbonated ashes must: (1) be 'fit for purpose' by conforming to an agreed specification, (2) be risk managed, and (3) meet a market need.

After each successive cycle of exposure to carbon dioxide gas, a gradual increase in the amount of CO₂ uptake was observed (Fig. 1, Table S1).

The potential of ashes to mineralise CO₂ was calculated theoretically, using the Steinoor equation⁶⁶. This equation uses the stoichiometry of an ash (taken from its oxide composition) to predict the maximum possible carbon 'uptake' as a % w/w (total weight). However, it should be noted that this equation and modifications thereof are not appropriate to all potentially carbonate-able wastes and the predictions are normally much more than can be achieved under laboratory/real-world conditions. The theoretical CO₂-uptakes in w/w (total weight) in shell, fibre and soft peel ashes were 26–45%, 4–55% and 28–49%, respectively (Fig. 2, Table S2). However, the experimental values recorded after 24 h of CO₂ exposure were indeed much less, being 9.9–15.6%, 25–29.4% and 5.6–24.17% w/w (total weight) in shell, fibre and soft peel ashes, respectively (Fig. 2, Table S2).

The crystalline phases observed in biomass ash included calcium oxide (CaO) and portlandite (Ca(OH)₂). Calcium oxide and portlandite are the major elements responsible for reaction with CO₂ under appropriate hydration condition. Hydration of CaO to portlandite (Ca(OH)₂) is an extremely exothermic reaction (– 104 kJ/mol)⁶⁷. On exposure to CO₂, portlandite forms calcium carbonate (CaCO₃) and this is similarly exothermic (– 32 kJ/mol)⁶⁸, which liberates the formerly bound water^{68,69}. Generally, > 10% w/w (total weight) of CaO in a material is associated with a CO₂ uptake that leads to hardening by self-cementation via calcium carbonate formation.

Nam et al. (2012)⁶⁶ suggest that as CO₂ becomes imbibed, the reaction is predominantly controlled by the phase-boundary, whereas later on, it is controlled by the diffusion of CO₂ through the surface carbonation reaction product. For fresh Portland cement, carbonation is essentially completed in three distinct phases involving 8 steps^{66,70}. With respect to biomass ash, no pre-treatment was required, and the carbonation reaction involved: gaseous CO₂ diffusing and dissolving into the film of moisture present on ash particles, followed by ionisation to HCO₃[–]. As the pH of the moisture film (which now contains dissolved CaO) falls, as it is neutralised, CaCO₃ is precipitated on the surface of ash particles, in pore space around and within the relict plant structures preserved

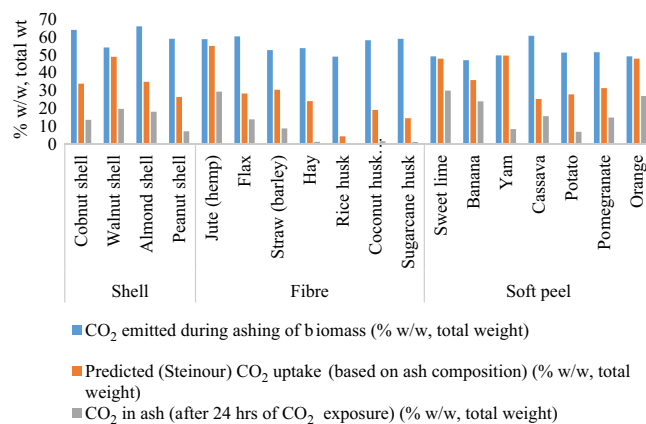


Figure 2. Theoretical and experimental CO₂ uptake in biomass ashes.

in the ash. The formation of carbonate causes cementation of adjacent ash particles and the infilling of void space to produce a hardened monolithic product (see Fig. 3).

The observed maximum CO₂ uptake was in ashes with the highest calcia content in the following order (low to high): jute (hemp), sweet lime, orange, banana and cassava peel, almond, walnut and cobnut shell, with a range from 10.43 to 29.45% w/w (total weight) (Fig. 2; Table S2). The calcia in these ashes was between 10.43 and 45.38% w/w (total weight), respectively (Table 3).

Carbon dioxide mineralisation of biomass ash was confirmed by X-Ray diffractometry by the presence of calcite. Rietveld refinement showed the relative occurrence of the major mineral phases in the biomass ashes and in their carbonated counterparts. As might be expected, the mineralogy of the ashes varied between the different biomass feedstock (Table 3). It should be noted that the mineralogy of the ashes is complex, and many amorphous phases are present. As such, the intensity of X-ray reflections is often lower than those obtained for mineral ashes from inorganic feedstock.

When exposed to CO₂ the ashes contained, for example, calcite and monohydrocalcite (observed for lime peel and nutshell). This clearly indicated that CO₂ had been mineralised, and calcium carbonate was formed within the range: 14–67% w/w (total weight). For the sake of brevity, main phases taken from diffractograms of the ‘raw’ ash and its carbonated counterpart are presented for each category of biomass examined (Table 4).

The minor presence of portlandite and/or CaO was noted in some of the carbonated ashes indicating that complete carbonation had not been fully achieved, and that further exposure to CO₂ was required. Some of the peel-derived ashes, such as banana and pomegranate were hygroscopic in nature and this could be attributed to the presence of sylvite (KCl); a phase that absorbs moisture from the air⁷¹. Portlandite development is also responsible for water sensitivity/expansion (and a relative loss of strength in carbonated monolithic specimens) when partially carbonated samples are immersed in water or exposed to the atmosphere⁷².

The literature has much information on the management of biomass ash and its effect on soil properties^{73–75}, not least as a way of replenishing essential nutrients and for modifying soil structure/microstructure. The very nature of plants to accumulate metals shows there is a key relationship between soil chemistry/mineralogy and the ‘needs’ of individual plants. Where calcium is concerned, a plant’s ability to accumulate this divalent metal can result in ash that readily carbonates on exposure to CO₂.

As mentioned, the uptake of CO₂ in the biomass ashes was related to presence of CaO arising from the high ashing temperature of 900 ± 25 °C. The mineralisation of CO₂ in the ashes was aided by their finely divided nature/high surface area, as noted by Castel et al. (2016)⁷⁶ and Filho et al. (2009)⁷⁷. Possan et al. (2017)⁷⁸ reported that CO₂ uptake by, for example, mixed wood ash blended with coal is largely regulated by particle surface area. However, particle size is not always the limiting factor for the CO₂ up taken, as is seen in our study. The findings of Nam et al. (2012)⁶⁶ involving municipal solid waste ash showed the amount of CO₂ sequestered increased as particle size decreased. This may well be valid for ashes with a similar chemistry, but where the amount of calcia varies in a feedstock (as seen in the present work) particle size, and in some cases, surface area may be secondary considerations.

Ash only monoliths. The CO₂ uptake in ‘ash-only’ monoliths (Table 5) showed that walnut shell, jute (hemp) and sweet lime peel reacted with the most CO₂ in their respective categories. However, as noted, a small amount of residual CaO in banana peel ash caused water sensitivity-related micro-cracking as calcia hydrated to portlandite, with a consequent increase in the volume.

Many of the biomass ashes studied have been shown to be very reactive to carbon dioxide gas forming calcium carbonate. The morphology of these carbonate products was examined using polished sections subject to backscattered electron microscopy. The spatial distribution of carbonate seen in the backscattered electron-micrographs suggests the nature of the individual biomasses may have an influence.

Three of the biomass residues, representing one type from each category studied, are given in Fig. 3a–c to illustrate the distinct morphology and carbonate distribution within the cemented biomass-ash monoliths. The observations made are summarised in each respective figure.

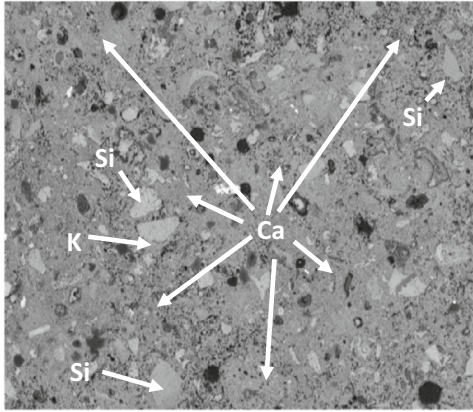
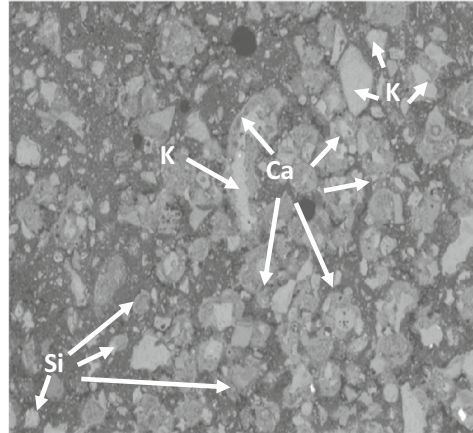
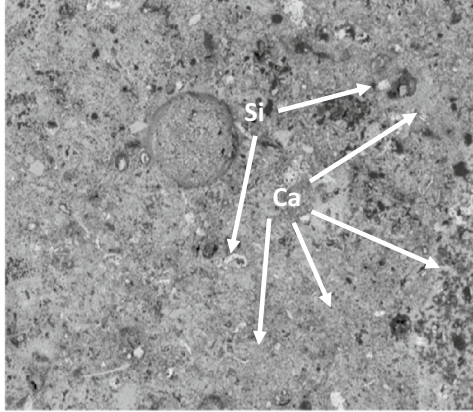
<p style="text-align: center;">Sweetlime peel carbonated 5</p>  <p style="text-align: center;">500µm</p> <p>(a)</p>	<p>The microstructure of carbonated sweet lime peel monolith shows sub-angular lime peel grains that are relatively uniform in nature, enveloped by groundmass that is generally microporous. Larger distinct isolated spherical voids (typically 3 to 10 µm) are common. EDS shows that calcium is uniformly distributed throughout, individual grains and matrix, however the former tend to be Silica rich and potassium poor. Relict structures originating from the peel were occasionally observed.</p>
<p style="text-align: center;">Almond shell carbonated 3</p>  <p style="text-align: center;">500µm</p> <p>(b)</p>	<p>Carbonated almond shell ash appeared well cemented, containing little observable porosity. A small number of spherical pores ca. 2% v/v appeared black in colour, and ranged in size from <5 µm to 100 µm. The matrix appeared darker (i.e. had a lower electron density) with individual angular to sub-rounded grains, (<250 µm) comprising ca. 50% v/v; often containing a lighter-coloured silica rich core, also associated with potassia and alumina. The darker outer portion of grains were Ca rich (an elongate grain, located upper centre left of the micrograph, this 'zoning'.</p>
<p style="text-align: center;">Hemp carbonated 1</p>  <p style="text-align: center;">500µm</p> <p>(c)</p>	<p>The microstructure of jute (hemp)-ash monoliths is unlike the others examined. A high proportion of relict-structures arising from the original biomass were observed which were not broken down during ashing. Small isolated lower porosity patches were observed in the matrix. Larger distinct grains were few, although one spherical grain (upper centre of micrograph) can be easily seen. Generally, calcia was found throughout the sample, but in angular ash particles, typically <125 µm, and more easily identified by their element composition (rather than by BSE), calcia and phosphorous occurred together.</p>

Figure 3. Back scattered micrographs and their descriptions (a) Sweet lime peel ash, (b) Almond shell ash and (c) Jute (hemp) ash.

The ashing of biomass at 900 ± 25 °C produced primarily CaO as the main calcium-bearing phase. Other minor phases including quartz and feldspar were also noted, which were present in the raw biomass or formed during ashing.

	Walnut shell	Jute (hemp)	Sweetlime peel
Lime (CaO)	–	–	–
Portlandite	33.07	–	–
Calcite	30.02	76.41	3.25
Monohydrocalcite	33.91	8.24	35.70
Hydroxylapatite	–	6.30	7.94

Table 4. Example major calcium containing phases in carbonated biomass ashes (%w/w, total weight) as determined by X-ray diffractometry. Data derived by Rietveld refinement; other phases detected included: periclase, quartz and feldspar.

'Ash-only' monolith		Density (g/cm ³)	CO ₂ uptake (g/kg)	Strength (MPa)	
				Carbonated	Uncarbonated
Shell	Cobnut shell	0.7	161.0	0.183	< 0.01
	Walnut shell	0.7	312.5	0.198	< 0.01
	Almond shell	0.7	342.0	0.507	< 0.01
	Peanut shell	0.4	156.2	0.169	< 0.01
Fibre	Jute (hemp)	0.5	325.0	0.147	< 0.01
	Flax	0.5	153.1	0.100	< 0.01
	Straw (barley)	0.5	78.0	0.161	< 0.01
	Hay	0.4	81.0	0.084	< 0.01
	Rice husk	0.2	– 9.95	0.028	< 0.01
	Coconut husk (coir)	0.4	20.5	– (Not cemented)	–
	Sugarcane husk	0.7	29.3	0.047	< 0.01
Soft peel	Sweet lime	0.6	283.0	0.313	< 0.01
	Banana	0.4	199.5	0.041	< 0.01
	Yam	0.4	136.8	0.022	< 0.01
	Cassava	0.5	147.0	0.256	< 0.01
	Potato	0.4	155.0	0.214	< 0.01
	Pomegranate	0.5	179.0	0.157	< 0.01
Orange	0.6	273.0	0.299	< 0.01	

Table 5. Mechanical properties of biomass ash monoliths.

It was also noted that monohydrocalcite was formed in combination with calcite during carbonation. Monohydrocalcite is a metastable phase which can transform to calcite or aragonite under the right environmental conditions. However, small amounts of phosphate can significantly inhibit transformation, and may explain why some of the samples contained both hydroxylapatite and monohydrocalcite⁷⁹. An example diffractogram showing these phases is given in Fig. 4.

Overall, the biomass ashes investigated were CO₂ reactive, and displayed a self-cementing capacity resulting in a hardened mineralised material. Interestingly, the variations in the microstructure of the mineralised products readily confirms carbonate cementation upon reaction with CO₂ gas. Furthermore, the possibility of achieving carbon balance/neutrality in the encapsulated biomass residues with sequestered CO₂ is established.

Raw biomass and ash monoliths. The embodied carbon calculated in monoliths produced from raw biomass combined with CO₂-reactive biomass ashes was 10–20% w/w (total weight). For cement-bound composites the amount measured was 10% w/w (total weight), clearly indicating (that despite containing the cement), the monoliths were carbon negative (Table 6). The mechanical properties of the ash + raw biomass-only monoliths without cement were inferior to those containing cement.

When the CO₂-reactive biomass ashes were used as a partial replacement for cement (see Table 6), it is possible to obtain respectable strengths and a reduced carbon footprint for the products formed. This particular part of our wider study will be published separately.

Strength of carbonated monolith samples

The carbonated 'ash only' monolithic cylinders were examined for their unconfined compressive strength and density (Table 5). The strength achieved was greatest for almond shell, straw and sweet lime in their respective categories. As compared to uncarbonated monolithic samples, all the carbonated biomass ashes were stronger. The monoliths made from rice and sugarcane husks, and yam peel recorded the lowest strengths, and this

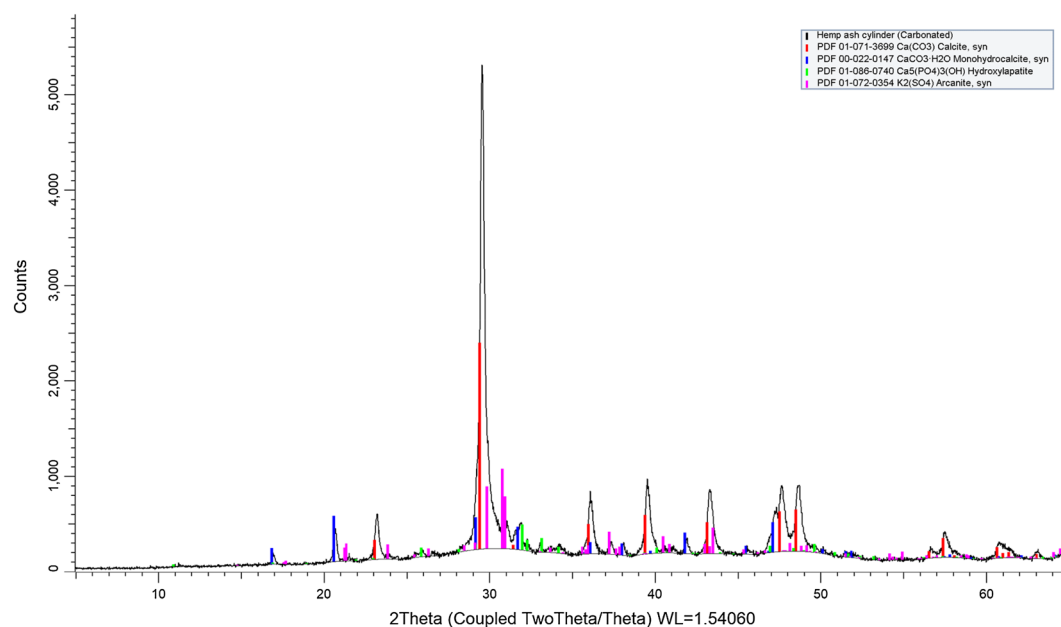


Figure 4. X-ray diffractogram showing polymorphs of carbonate in carbonated hemp ash cylinder/monolith.

Combinations	Density of valorised raw biomass and ash products (carbonated) (g/cm ³)	Strength of valorised raw biomass and ash products (carbonated) (MPa)	CO ₂ in valorised raw biomass and ash products (1-week carbonation) (%)
Orange peel + cement (20%) + sand (10%)	400	0.230	45.1
Orange peel + Poplar shavings ash, cement and sand (10% each)	350	0.160	43.6
Hazelnut shell + cement (20%) + sand (10%)	880	0.450	28.6
Hazelnut shell + Hazelnut shell ash, cement and sand (10% each)	740	0.280	26.4

Table 6. Mechanical properties of a few biomass ash containing raw biomass monoliths (Tripathi and Hills et al. 2020)⁵⁴.

appears to be related to raised silica content (15–65% w/w, total weight). Interestingly, coconut husk ash poorly self-cemented (despite having a modest silica content) and this was attributed to the formation of sylvite (KCl) in the hardened product.

In most of the cases, the uptake of CO₂ in ashes corresponded to the strength recorded for the carbonate cemented monoliths (i.e. higher CO₂ uptake = higher strength). However, in some cases, e.g., for banana peel a high CO₂ uptake resulted in a low recorded strength; here being attributed to incomplete carbonation leading to mild expansion and microcracking (Fig. 5).

As a means of comparing how the strengths of the small monolithic specimens made from carbonated biomass ash with commercially manufactured carbonated products reference is made to the European standard for lightweight aggregates⁸⁰. It was found that the strength of all the carbonated ash-monoliths examined exceeded the strength criteria given in this standard, being an average of 0.1 MPa. This strength is also that required for 'end of waste' approval for UK commercially available manufactured carbonated aggregate-products, made from CO₂ reactive inorganic wastes⁸¹.

Implications

Some of the nutshell, fibre and soft peel ashes have displayed potential to combine with ca. 25% of their own weight of CO₂. However, most of the fibre-ashes captured much less CO₂. Nevertheless, the amount of captured CO₂ is the direct offset of the CO₂ emitted during ashing.

The development of strength by self-cementation by carbonate formation may not necessarily be sufficient for biomass ash raw-biomass composites to be employed as building materials. Under these circumstances a more 'potent' carbonate-able binder may be used, and Portland cement is one such binder.

As shown in this work, when Portland cement is used as a carbonate-able binder, replacement by biomass ash can be used to increase the embodied carbon in the product whilst maintaining desirable strength characteristics. It is worthy of note from our earlier work⁵⁴, Ca-rich biomass ash from woody feedstock could be used to partially replace Portland cement in a hydraulic system without loss of product strength, providing flexibility in approach.

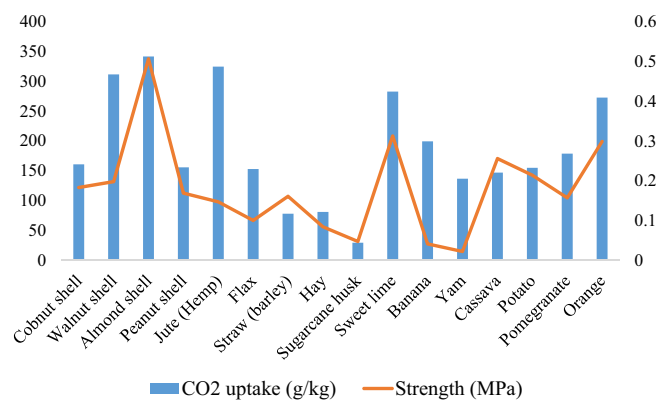


Figure 5. Relationship between strength and CO₂ uptake in monoliths from biomass residues.

The strengths observed for biomass ash monoliths and our reference cement-bound samples ranged between 160 and 450 kPa. Considering that the composites were raw biomass at 70% w/w (total weight), these strengths were enough for the samples to be robustly handled. There is also a considerable amount of embodied carbon in these composite products, ranging between 26 and 45% w/w (total weight).

An emission factor for CO₂ emissions from burning of crop residues has been calculated as 1585 g/kg by Akagi et al. (2011)⁸². However, under the laboratory conditions used in this work, we calculated the emissions from burning of crop residues to be 47–66% w/w (total weight) CO₂, which is lower than that reported by these authors using a CO₂ equivalent calculation.

The direct offset of CO₂ emissions after carbonation of ashes (i.e. what was mineralised/in the raw biomass) could be calculated based on the CO₂ mineralised the products.

The indirect offset, when Portland cement is used (as a carbonate-able binder), can be calculated through the reduction in use of cement by partial replacement by biomass ash. Further potential benefits include release of land space currently used for dumping biomass residues.

A simplified conceptual diagram shown in Fig. 6 delineates the offset options for CO₂ emission by using our low carbon CCUS approach for the valorisation of selected biomass waste. This diagram, however, does not consider the energy involved in burning biomass, as that is the part of a separate study. Nevertheless, direct and indirect offsets calculated for selected biomass residues amount to 134 Mt of CO₂/year.

Conclusion

The ‘proof of concept’ established through this study shows that the residual ash from the burning of certain agricultural biomass waste contains enough calcium oxide ($\times 100$ g/kg), to enable carbonate-hardened monolithic products to be manufactured on exposure to CO₂ gas. A negative relationship between calcia content and ash yield was identified. When fully carbonated, these small monolithic products similar in size to manufactured carbonated aggregate are resistant to water and have acceptable strength, as specified in the European standard for light-weight aggregates, BSEN 13055:2016.

These findings suggest an alternative ‘low carbon’ route for biomass waste utilisation is potentially available, which can sequester significant ($\times 100$ Mt) amounts of CO₂ in products with value.

We conclude from this study that there are a number of significant potential benefits from utilising biomass waste ash that has been mineralised:

- significant amounts of CO₂ can be permanently stored, being up to 29.5% w/w, total weight
- processing can be carried under ambient conditions opening up the possibility of using point-source emissions at low cost
- ashes readily self-cement and the products have MPa strength, and appear environmentally stable
- biomass ash wastes normally disposed to landfill under waste management regulations have a route for valorisation via ‘end of waste’
- the combining of solid and gaseous wastes in products is a circular economic activity with significant potential sustainability gains
- The combined direct and indirect CO₂ offset was calculated as 134 Mt/year for the selected biomass residues (incl. crop, fruit and vegetable waste); this amount is equivalent to, e.g., nearly 40% of the UK’s GHG emissions predicted for 2019.

Received: 2 April 2020; Accepted: 27 July 2020

Published online: 14 August 2020

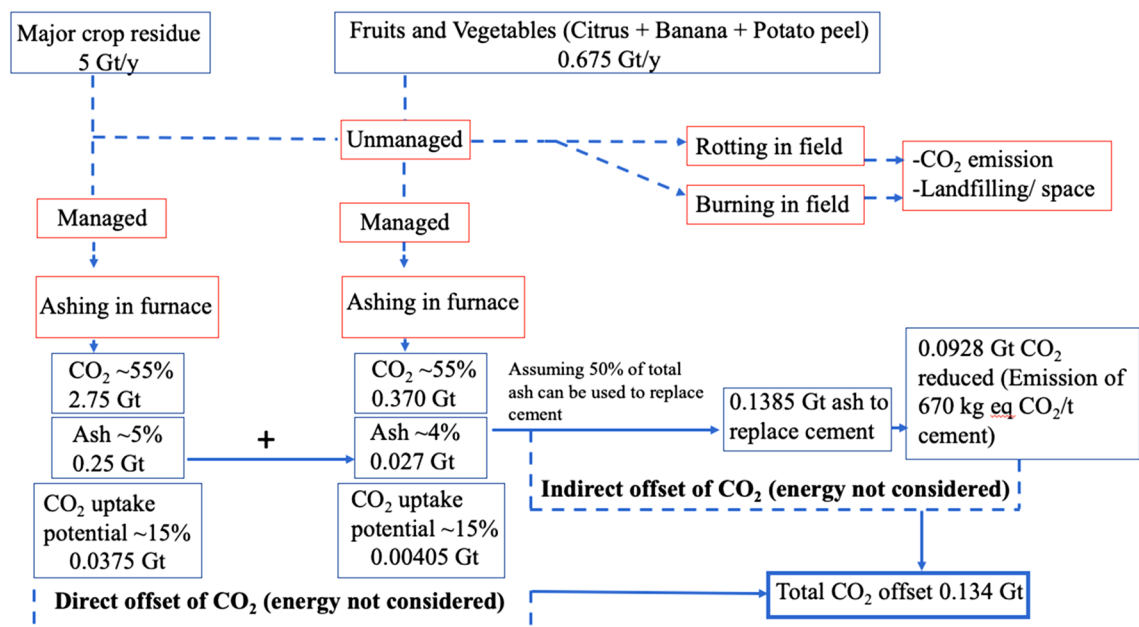


Figure 6. A conceptual diagram for CO₂ emission offset envisaged from CCUS option for biomass waste valorisation.

References

- PBL Netherlands Environmental Assessment Agency Report. Integrated analysis of global biomass flows in search of the sustainable potential for bioenergy production. *PBL Publication* no. 1509. <https://www.pbl.nl/sites/default/files/cms/publicaties/pbl-2014-integrated-analysis-of-global-biomass-flows-in-search-of-the-sustainable-potential-for-bioenergy-production-1509.pdf> (2014)
- UNEP (United Nations Environment Programme) Converting waste agricultural biomass into a resource. United Nations Environment Programme Division of Technology, Industry and Economics International Environmental Technology Centre, Osaka/Shiga, Japan. www.unep.org/ietc/Portals/136/Publications/Waste%20Management/WasteAgriculturalBiomassEST_Compndium.pdf (2015)
- Nakamura, T. Waste Agriculture Biomass Convention, the 6th Biomass Asia Workshop in Hiroshima, 18–20 November 2009, IETC Osaka, https://www.biomass-asia-workshop.jp/biomassws/06workshop/presentation/25_Nakamura.pdf, New York Times dates 5 August 2010, New York (2009)
- Centore, M., Hochman, G. & Zilberman, D. Worldwide survey of biodegradable feedstocks, waste-to-energy technologies, and adoption technologies. In *Modelling, Dynamics, Optimization and Bioeconomics I. Springer Proceedings in Mathematics and Statistics*, Vol. 73 (eds Pinto, A. A. & Zilberman, D.) (Springer, Berlin, 2014). https://doi.org/10.1007/978-3-319-04849-9_11.
- Lal, R. World crop residues production and implication of its use as a biofuel. *Environ. Int.* **31**(4), 575–584 (2019).
- IEA. International Energy Agency, CCC World forest and agricultural crop residue resources for co-firing. ISBN 978-92-9029-571-6 (2015) https://www.usea.org/sites/default/files/042015_World%20Forest%20and%20agricultural%20crop%20residue%20resources%20for%20cofiring_ccc249.pdf
- FAO. World agriculture: towards 2015/2030. *Summary Report* ISBN 92-5-104761-8 (2002). <https://www.fao.org/3/a-y3557e.pdf>; <https://www.fao.org/docrep/004/y3557e/y3557e04.htm#TopOfPage>
- FAO. World Agriculture Towards 2030/2050: The 2012 revision *ESA E Working Paper No. 12-03* (2012) https://www.fao.org/fileadmin/user_upload/esag/docs/AT2050_revision_summary.pdf
- Slade, R., Saunders, R., Gross, R. & Bauen, A. Energy from biomass: the size of the global resource. An assessment of the evidence that biomass can make a major contribution to future global energy supply. *Imperial College Centre for Energy Policy and Technology and UK Energy Research Centre*, London ISBN: 1 903144 108 (2012)
- Bentsen, N. S. & Felby, C. Technical potentials of biomass for energy services from current agriculture and forestry in selected countries in Europe, The Americas and Asia. *Forest & Landscape Working Papers* No. 54, 31 pp. Forest & Landscape Denmark, Frederiksberg (2010)
- FAO FAOSTAT. *UN Food and Agricultural Organization*, Roma, Italy (2014) <https://faostat.fao.org/site/567/DesktopDefault.aspx?PageID=567#ancor> or https://faostat3.fao.org/browse/Q/*E
- Haberl, H., Beringer, T., Bhattacharya, S. & Erb, K. H. The global technical potential of bioenergy in 2050 considering sustainability. *Curr. Opin. Environ. Sustain.* **2**(5–6), 394–403 (2010).
- Yamamoto, H., Fujino, J. & Yamaji, K. Evaluation of bioenergy potential with a multi-regional global land-use-and-energy model. *Biomass Bioenergy* **21**, 185–203 (2001).
- Lal, R. World crop residues production and implications of its use as a biofuel. *Environ. Int.* **31**, 575–584 (2005).
- Krausmann, F., Erb, K. H., Gingrich, S., Lauk, C. & Haberl, H. Global patterns of socioeconomic biomass flows in the year 2000: a comprehensive assessment of supply, consumption and constraints. *Ecol. Econ.* **65**(3), 471–487 (2008).
- Smeets, E. M. W., Faaij, A. P. C., Lewandowski, I. M. & Turkenburg, W. C. A bottom-up assessment and review of global bio-energy potentials to 2050. *Prog. Energy Combust. Sci.* **33**(1), 56–106 (2007).
- Bentsen, N.S. & Felby, C. Technical potentials of biomass for energy services from current agriculture and forestry in selected countries in Europe, the Americas and Asia. In *Working Papers/Forest & Landscape. Copenhagen, DK: Forest & Landscape Denmark* **31** (2010)
- Smeets, E., Faaij, A. & Lewandowski, I. A. quick scan of global bio-energy potentials to 2050. An analysis of the regional availability of biomass resources for export in relation to the underlying factors. Report NWS-E-2004-119, March 2004. Utrecht University, Utrecht (2004)
- IRENA. *Global Bioenergy Supply and Demand Projections: A working paper for Remap 2030* (2014)

20. Smil, V. Nitrogen in crop production. *Glob. Biochem. Cycles* **13**(2), 647–662 (1999).
21. Sanginga, N. & Mbabu, A. Root and Tuber Crops (Cassava, Yam, Potato and Sweet Potato). Feeding Africa. *Abdou Diouf International Conference Centre*. Dakar, Senegal (2015)
22. FAO. World agriculture: towards 2030/2050. Interim report. *Prospects for food, nutrition, agriculture and major commodity groups* (2006)
23. United Nations Economic Commission for Africa. Root and tuber crops (cassava, yam, potato and sweet potato). An Action Plan for African Agricultural Transformation. Background Paper. *United Nations Economic Commission for Africa* (2015) <https://pdfs.semanticscholar.org/8330/8566f9e3d22c937eca9cfd6b83a24583742.pdf>
24. FAO. The State of Food Insecurity in the World. Economic growth is necessary but not sufficient to accelerate reduction of hunger and malnutrition. *World Food Programme (WFP) & International Fund for Agricultural Development (IFAD)* (2012)
25. FAO, IFAD and WFP. The State of Food Insecurity in the World 2015. Meeting the 2015 international hunger targets: taking stock of uneven progress. Rome, FAO (2015) <https://www.fao.org/3/a-i4646e.pdf>
26. Monfreda, C., Ramankutty, N. & Foley, J. A. Farming the planet: 2. Geographic distribution of crop areas, yields, physiological types, and net primary production in the year 2000. *Glob. Biogeochem. Cycles* **22**, 1022 (2008).
27. Mendu, V. *et al.* Identification and thermochemical analysis of high-lignin feedstocks for biofuel and biochemical production. *Biotechnol. Biofuels* **4**, 43. <https://doi.org/10.1186/1754-6834-4-43> (2011).
28. Warren, J. *The Nature of Crops: How We Came to Eat the Plants We Do*. CAB International. ISBN-13:978 1 78064 508 7. www.cabi.org (2015)
29. The Hindu. With 98% cashew apple going to waste, traders look for alternative use (2014) <https://www.thehindubusinessline.com/economy/agri-business/With-98-cashew-apple-going-waste-traders-look-for-alternative-use/article20887136.ece>
30. IEA. Tracking Industry. IEA, Paris (2019) <https://www.iea.org/reports/tracking-industry-2019>
31. Statista. Major countries in worldwide cement production from 2012 to 2017 (in million metric tons) (2018) <https://www.statista.com/statistics/267364/world-cement-production-by-country/>
32. IEA, International Energy Agency, CCC World forest and agricultural crop residue resources for co-firing. ISBN 978-92-9029-571-6 (2015). https://www.usea.org/sites/default/files/042015_World%20Forest%20and%20agricultural%20crop%20residue%20resources%20for%20cofiring_ccc249.pdf
33. Jain, N., Pathak, H. & Bhatia, A. Sustainable management of crop residues in India. *Curr. Adv. Agric. Sci.* **6**(1), 1–9 (2014).
34. Devi, S., Gupta, C., Jat, S. L. & Parmar, M. S. Crop residue recycling for economic and environmental sustainability: the case of India. *Open Agric.* **2**, 486–494 (2017).
35. Mandavgane, S. A., Pathak, P. D. & Kulkarni, B. D. Fruit peel waste: characterization and its potential uses. *Curr. Sci.* **113**, 3 (2017).
36. Tripathi, N., Hills, C. D., Singh, R. S. & Atkinson, C. J. Biomass waste utilisation in low-carbon products: harnessing a major potential resource. *NPJ Clim. Atmos. Sci.* **2**, 35 (2019).
37. Berndes, G., Hoogwijk, M. & van den Broek, R. The contribution of biomass in the future global energy supply: a review of 17 studies. *Biomass Bioenergy* **25**, 1–28 (2003).
38. Hamelinck, C. & Hoogwijk, M. *Future Scenarios for First- and Second-Generation Biofuels* (Ecofys, Utrecht, 2007).
39. Dornburg, V. *et al.* Bioenergy revisited: key factors in global potentials of bioenergy. *Energy Environ. Sci.* **3**, 258–267 (2010).
40. Chum, H. & Faaij, A. & Moriera, J., *et al.* Bioenergy. In *IPCC Special Report on Renewable Energy Sources and Climate Change Mitigation* (eds Edenhofer, O. *et al.*) 209–331 (Cambridge University Press, Cambridge, 2011).
41. Searle, S. & Malins, C. A. Reassessment of global bioenergy potential in 2050. *GCB Bioenergy* **7**, 328–336 (2014).
42. UNEP, Converting Waste Agricultural Biomass into a Resource. UNEP Compendium of Technologies (2009) https://www.unep.org/ietc/Portals/136/Publications/Waste%20Management/WasteAgriculturalBiomassEST_Compendium.pdf
43. World Energy Outlook. Energy poverty: How to make modern energy access universal? In *World Energy Outlook 2010* for the UN General Assembly on the Millennium Development Goals. Paris, Organisation for Economic Co-operation and Development & International Energy Agency (2010)
44. Amegah, A. K. & Jaakkola, J. K. Household air pollution and the sustainable development goals. *Bull. World Health Organ.* **94**, 215–221. <https://doi.org/10.2471/BLT.15.155812> (2016).
45. Batchelor, S., Brown, E., Scott, N. & Leary, J. Two birds, one stone—reframing cooking energy policies in Africa and Asia. *Energies* **12**, 1591. <https://doi.org/10.3390/en12091591> (2019).
46. ECN, Biomass Waste-to-Energy Toolkit for Development Practitioners (2014) <ftp://ftp.ecn.nl/pub/www/library/report/2014/o14054.pdf>. Accessed 06 June 2020.
47. EPRS. European Parliamentary Research Service. *Members' Research Service* PE 568.329 (2015)
48. Armstrong, K. & Styring, P. Assessing the potential of utilization and storage strategies for post-combustion CO₂ emissions reduction. *Front. Energy Res.* <https://doi.org/10.3389/fenrg.2015.00008> (2015).
49. IPCC. Summary for Policymakers of IPCC. *Special Report on Global Warming of 1.5°C approved by governments* (2018). https://www.ipcc.ch/newsandevents/pr181008_P48_spm.shtml
50. <https://www.theguardian.com/world/2019/nov/05/india-top-court-orders-halt-to-stubble-burning-to-cut-delhi-pollution>
51. Claisse, P. A. Introduction to cement and concrete. *Civ. Eng. Mater.* <https://doi.org/10.1016/B978-0-08-100275-9.00017-6> (2016).
52. Bertos, M. F., Simons, S. J. R., Hills, C. D. & Carey, P. J. A review of accelerated carbonation technology in the treatment of cement-based materials and sequestration of CO₂. *J. Hazard. Mater.* **112**, 193–205 (2004).
53. Flannery, T. A. 'Third Way' to Fight Climate Change. The opinion pages. *New York Times* (2015). https://www.nytimes.com/2015/07/24/opinion/a-third-way-to-fight-climate-change.html?_r=0
54. Tripathi, N., Hills, C. D., Singh, R. S. & Singh, J. S. Offsetting anthropogenic carbon emissions with novel materials from biomass waste and mineralised carbon dioxide. *Sci. Rep.* **10**, 958 (2020).
55. Andrews, R. Global CO₂ emissions from cement production. *Earth Syst. Sci. Data* **10**, 195–217 (2018).
56. Vassilev, S. V., Vassileva, C. G., Song, Y. C., Li, W. Y. & Feng, J. Ash contents and ash-forming elements of biomass and their significance for solid biofuel combustion. *Fuel* **208**, 377–409 (2017).
57. Sweitzer, J. Five calcium rich fruits for healthy teeth. *Cirocco Dental Center* (2018) <https://www.ciroccodentalcenterpa.com/food/5-calcium-rich-fruits-for-healthy-teeth/>
58. Kuhad, R. C. & Singh, A. *Biotechnology for Environmental Management and Resource Recovery* (Springer, Berlin, 2013). ISBN 978-81-322-0875-4.
59. Vassilev, S., Baxter, D., Andersen, L. K. & Vassileva, C. G. An overview of the composition and application of biomass ash. Part 2. Potential utilisation, technological and ecological advantages and challenges. *Fuel* **105**, 19–39 (2013).
60. Vassilev, S. V., Vassileva, C. G. & Baxter, D. Trace element concentrations and associations in some biomass ashes. *Fuel* **129**, 292–313 (2014).
61. Monti, A., Di Virgilio, N. & Venturi, G. Mineral composition and ash content of six major energy crops. *Biomass Bioenergy* **32**, 216–223 (2008).
62. Paulrad, S., Nilsson, C. & Öhman, M. R. Reed canary grass ash composting and its melting behaviour during combustion. *Fuel* **80**, 1391–1398 (2001).
63. Sander, B. Properties of Danish biofuels and the requirements for power production (ELSAMPROJEKT A/S). *Biomass Bioenergy* **12**(3), 177–183 (1997).

64. Prade, T., Finell, M., Svensson, S. E. & Mattsson, J. E. Effect of harvest date on combustion related fuel properties of industrial hemp (*Cannabis sativa* L.). *Fuel* **102**, 592–604 (2012).
65. Jørgensen, U. & Sander, B. Biomass requirements for power production: how to optimise the quality by agricultural management. *Biomass Bioenergy* **12**, 145–147 (1997).
66. Nam, S. Y., Seo, J., Thriveni, T. & Ahn, J. W. Accelerated carbonation of municipal solid waste incineration bottom ash for CO₂ sequestration. *Geosyst. Eng.* **15**(4), 305–311 (2012).
67. Criado, Y. A., Alonso, M. & Abanades, J. C. Kinetics of the CaO/Ca(OH)₂ hydration/dehydration reaction for thermochemical energy storage applications. *Ind. Eng. Chem. Res.* **53**, 12594–12601 (2014).
68. Montes-Hernandez, G., Renard, F., Geoffroy, N., Charlet, L. & Pironon, J. Calcite precipitation from CO₂-H₂O-Ca(OH)₂ slurry under high pressure of CO₂. *J. Cryst. Growth* **308**, 228–236 (2007).
69. Sarenbo, S., Mellbo, P., Stålnacke, O. & Claesson, T. Reactivity and leaching of wood ash pellets dehydrated by hot air and flue gas. *Open Waste Manag. J.* **2**, 47–54 (2009).
70. Maries, A. The activation of portland cement by carbon dioxide. In *Proceedings of Conference in Cement and Concrete Science*, Oxford, UK (1985).
71. NSRDS. Physical properties data for rock salt. *National Bureau of Standards Monograph* **167**, 288 pp. CODEN: NBSMA6 (1981).
72. Gagné, R. Expansion due to the formation of portlandite. In *Science and Technology of Concrete Admixtures* (eds Aïtcin, P.-C. & Flatt, R. J.) (Elsevier, New York, 2016). ISBN 978-0-08-100693-1.
73. James, A. K., Thring, R. W., Helle, S. & Ghuman, H. S. Ash management review-applications of biomass bottom ash. *Energies* **5**, 3856–3873 (2012).
74. Knapp, B. A. & Insam, H. Recycling of biomass ashes: current technologies and future research needs. In *Recycling of Biomass Ashes* (eds Insam, H. & Knapp, B. A.) 87–105. <https://doi.org/10.1007/978-3-642-19354-5> (2011)
75. Okmanis, M., Lazdia, D. & Lazdi, A. A. The composition and use value of tree biomass ash. *Rural Sustain. Res.* **34**, 329. <https://doi.org/10.1515/plua-2015-0011> (2015).
76. Castel, Y., Amziane, S. & Sonebi, M. Durabilité du béton de chanvre: résistance aux cycles d’immersion hydrique et séchage, lère Conférence EuroMaghrébine des BioComposites, Marrakech 28–31 March (2016)
77. Filho, R. D. T., Silva, F. D. A., Fairbairn, E. M. R. & Filho, J. D. A. M. Durability of compression molded sisal fiber reinforced mortar laminates. *Constr. Build. Mater.* **23**(6), 2409–2420 (2009).
78. Possan, E., Thomaz, W. A., Aleandri, G. A., Felix, E. F. & Santos, A. C. P. CO₂ uptake potential due to concrete carbonation: a case study. *Case Stud. Constr. Mater.* **6**, 147–161 (2017).
79. Fukushi, K., Munemoto, T., Sakai, M. & Yagi, S. Monohydrocalcite: a promising remediation material for hazardous anions. *Sci. Technol. Adv. Mater.* **12**(6), 064702 (2011).
80. BSEN 13055. Lightweight aggregates (2016) <https://www.thenbs.com/PublicationIndex/documents/details?Pub=BSI&DocID=314445>
81. Gunning, P. J., Antemir, A., Hills, C. D. & Carey, P. J. Secondary aggregate from waste treated with carbon dioxide. *Proc. Inst. Civ. Eng. Constr. Mater.* **164**, 231–239 (2011).
82. Akagi, S. K. *et al.* Emission factors for open and domestic biomass burning for use in atmospheric models. *Atmos. Chem. Phys.* **11**, 4039–4072 (2011).
83. FAO. FAO Statistics Data 2014. www.fao.org/faostat/en/#data (2017)
84. Gupta, K. & Joshi, V. K. Fermentative utilization of waste from food processing industry. In *Postharvest Technology of Fruits and Vegetables: Handling, Processing, Fermentation and Waste Management* (ed. Joshi, V. K.) 1171–1193 (Indus Pub Co, New Delhi, 2000).
85. Saxena, A., Bawa, A. S. & Raju, P. S. Jackfruit (*Artocarpus heterophyllus* Lam.). In *Postharvest Biology and Technology of Tropical and Subtropical Fruits* (ed. Yahia, E. M.) 275–298 (Woodhead Publishing Limited, Cambridge, 2011).
86. Sagar, N. A., Pareek, S., Sharma, S., Elhadi, M. Y. & Lobo, M. G. Fruit and vegetable waste: bioactive compounds, their extraction, and possible utilization. *Comprehensive Rev. Food Sci. Food Saf.* **17**, 512–531 (2018).

Author contributions

C.D.H., N.T. and R.S.S. conceptualised and designed the research work; N.T. performed the experiments; N.T. and C.D.H. jointly wrote the M.S.S.; P.C. and F.L. provided technical advise and reviewed the M.S.S.

Competing interests

The authors declare no competing interests.

Additional information

Supplementary information is available for this paper at <https://doi.org/10.1038/s41598-020-70504-1>.

Correspondence and requests for materials should be addressed to C.D.H. or N.T.

Reprints and permissions information is available at www.nature.com/reprints.

Publisher’s note Springer Nature remains neutral with regard to jurisdictional claims in published maps and institutional affiliations.



Open Access This article is licensed under a Creative Commons Attribution 4.0 International License, which permits use, sharing, adaptation, distribution and reproduction in any medium or format, as long as you give appropriate credit to the original author(s) and the source, provide a link to the Creative Commons license, and indicate if changes were made. The images or other third party material in this article are included in the article’s Creative Commons license, unless indicated otherwise in a credit line to the material. If material is not included in the article’s Creative Commons license and your intended use is not permitted by statutory regulation or exceeds the permitted use, you will need to obtain permission directly from the copyright holder. To view a copy of this license, visit <http://creativecommons.org/licenses/by/4.0/>.

© The Author(s) 2020